 Copyright 1999, IS&T

Mechanistic Statistical Study of the Speed Dependence of Magnetic Background

Jean-Jacques P. Eltgen
Nipson, a Xeikon Company
Belfort, France

Abstract

The mechanisms underlying the generation of magnetic background in magnetography are analyzed from the standpoint of random collisions between toner particles during development. Particles are supposed either already captive in non-image area, or still free in the developer bed. The outcome of collisions is determined by comparing the magnetostatic energy of the former type of particles, with the kinetic energy of the latter type. The critical process speed, at which background is minimum, depends on the imaging media permeability and the toner magnetic characteristics. The rate at which background decreases for sub-critical speeds is related to the particle size distribution and the number of collisions expected at each development position. Quantitative results from the model are shown to be fairly in agreement with experimental data.

Introduction

The effect of speed on background development in magnetography has been previously reported[1]. Experimental evidences are: (a) background exhibits a sharp rate of decrease with increasing speed, until a 'critical speed' u_c is reached; (b) above u_c, background resumes increasing, but at a lower rate. It was suggested that: (c) 'primary' background at sub-critical speed results from competition between magnetic self-attraction of pre-magnetized particles to the magnetic media and detachment force due to impacts with free particles in the developer bed; (d) 'secondary' background at super-critical speed stems from airborne particle re-deposition now dominating kinetic scavenging.

Hypothesis (c) was used in previous papers[2,3] to determine first order approximations of the performance range of magnetography. Speed-wise, the upper boundary to the operating range was just taken equal to the 'critical' speed u_c, with no consideration of the stochastic nature of the collision process.

The present paper provides deeper insights into the mechanisms of collisions between particles, by introducing the statistical distribution of toner particle size and the average number of shocks expected to occur at a given development position.

Mechanistic Aspect

Magnetostatic Energy

The magnetostatic energy density for a toner particle, assumed captive in the background, is expressed as[2]:

$$\frac{E_m}{V}=\frac{1}{12}\mu_0\frac{\mu-1}{\mu+1}\eta^2 {J_0}^2 \tag{1}$$

where E_m is the energy, V the toner particle volume, η the oxide volume fraction in the toner material, J_0 the oxide intrinsic magnetization, and μ the permeability of the media. μ_0 is vacuum permeability = $4\,\pi\,10^{-7}$ in SI units.

Escape Velocity

E_m is nothing but the work necessary to move the particle from its current location to an infinite distance from the medium where the force is zero. A mean of doing that is to give the particle, e.g., during a shock, a kinetic energy E_c at least equal to E_m.

This determines a minimum 'escape' velocity u_0 as:

$${u_0}^2=\frac{1}{6}\frac{\mu_0}{\rho_0}\frac{(\mu-1)}{(\mu+1)}\frac{\eta^2}{(1+4\eta)}{J_0}^2 \tag{2}$$

where ρ_0 is the toner polymer density, and we assume an oxide density typically 5 times larger.

Physically, if the particle is given a velocity lower than u_0, then it will fall back in the background; in the other case it will escape.

Elastic Shock

Let P1 be a particle of radius r captive in background, and P_2 another particle of radius R free in the developer bed. With reference to a coordinate system fixed to the media, P1 is static, while P2 has a velocity u, itself a direct function of the process speed.

If P2 (initial speed u) collides into P1 (initial speed 0), then classical mechanics yields the following speeds after the shock, assumed here perfectly elastic:

$$\text{P1}:\ u_1=\frac{2R^3}{R^3+r^3}u \qquad \text{P2}:\ u_2=\frac{R^3-r^3}{R^3+r^3}u \tag{3}$$

(the magnetostatic energy does not affect the solution since it is the same just before and just after the shock).

Critical Sizes

We now define, for each captive particle P1 of radius r, a number of critical sizes for the incident particle P2.

First, P1 will escape only if $u_1 > u_0$; i.e., using Eq. 2 and Eq. 3, if P2 has a minimum radius R_0:

$$R > R_0 = \sqrt[3]{\frac{u_0}{2u - u_0}}\ r \tag{4}$$

where R_0 exists only if: $u > u_0/2$. Therefore, for speeds lower than half the escape velocity, no captive particle can be scavenged. Alternatively, for speeds greater than half the escape velocity, there is a critical radius R_0 for the incident particle P2, such that P1 can be scavenged in one shock.

Second, we also have to consider what happens to P2 after the shock. Since Eq.3 can produce negative values of u_2, which physically corresponds to the case where P2 bounces backward, it is the absolute value $|u_2|$ that we have to compare to u_0. This defines two other boundary values R_1 and R_2 for the radius of P2:

$$R < R_1 = \sqrt[3]{\frac{u - u_0}{u + u_0}}\ r \qquad \text{or} \qquad \sqrt[3]{\frac{u + u_0}{u - u_0}}\ r = R_2 < R \tag{5}$$

and we note that R_1 and R_2 exist only if: $u > u_0$.

The critical values R_0, R_1, R_2 for the radius R of P2, normalized by the radius r of P1, are shown in Figure 1 as a function of the speed ratio u / u_0.

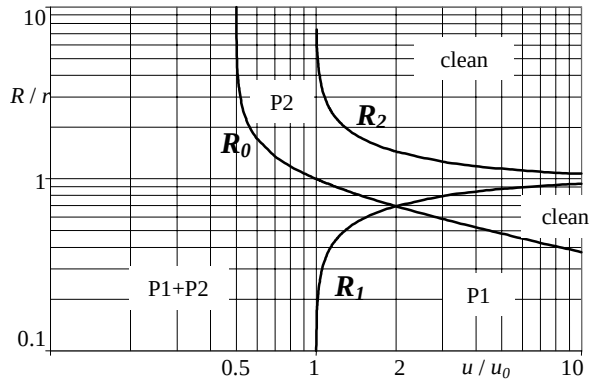

Figure 1. Normalized critical radii as a function of ratio u / u_0.

Modes of Operation

Examination of Figure 1 leads to the definition of 4 modes.

Mode 1: $u < u_0/2$; then none of R_0, R_1, R_2 exist and no captive particle can be scavenged. Background is instant. This is clearly a non-operating mode for magnetography.

Mode 2: $u_0/2 < u < u_0$; then only R_0 exists and a captive particle P1 can be scavenged by free particles P2 larger than R_0. But such P2 will themselves be trapped in background, so P1 is just being replaced by another particle P2 of larger size (since $R_0 > r$). Background may just increase in time as more collisions occur. This is also a non-operating mode.

Mode 3: $u_0 < u < 2u_0$; then all R_0, R_1, R_2 exist with ranking relation: $R_1 < R_0 < r < R_2$. Again, each captive particle P1, whatever its radius r, can be scavenged by free particles P2 of radius larger than R_0 (with now $R_0 < r$). But only larger P2, massive enough to retain enough momentum, can themselves escape background. Therefore, in this mode, the final status after one shock is one of 4 states: P1 only; P2 only; P1 and P2; no background.

Mode 4: $2u_0 < u$; all R_0, R_1, R_2 still exist with new ranking condition: $R_0 < R_1 < r < R_2$. The difference with Mode 3 is that background after one shock now takes one of only 3 states: P1 only; P2 only; no background.

In summary, only Modes 3 and 4 are operationg modes. We shall concentrate on these last two modes in the rest of this paper. At this point, we already note that $2u_0$, i.e., twice the escape speed, acts as a critical value separating two operating modes. We shall see later that it is nothing but the critical speed u_c experimentally observed.

Statistical Aspect

We now introduce the particle size distribution, defined by its probability density function $g(r)$. By definition, $g(r)dr$ represents the probability that the particle radius, considered as a random variable R, be comprised between r and $r+dr$:

$$\text{prob}\left[r \le R < r + dr\right] = g(r)dr \qquad \text{with :} \quad \int_0^\infty g(r)dr = 1 \tag{6}$$

and we classically assume for $g(r)$ a log-normal distribution:

$$g(r) = \frac{1}{r\tau\sqrt{2\pi}} e^{-\frac{(\ln r - \lambda)^2}{2\tau^2}} \tag{7}$$

Sub-Critical Speed

In Mode 3, the probability that P1 be detached in one collision is:

$$p_1(r) = \int_{R_2(r)}^{\infty} g(x)dx \tag{8}$$

where the function $R_2(r)$ is given by Eq. 5.

In reality, while passing through the developer bed, each given background position is exposed to a random number of collisions N, which mean value N^* is taken as:

$$N^* = \frac{L\,p}{2r^*} \tag{9}$$

where L is the length of the developer bed in the process direction, p is the toner compaction in the bed, and $r^* = \exp(\lambda + \tau^2/2)$ is the mean value of the particle radius for the distribution $g(r)$.

The sequence of N^* collisions consists of the repetition of a random event of probability p_1. It is therefore governed by the binomial probability law. In particular, for any background position assumed initially occupied by a captive particle of radius r and being exposed to an average number

of collisions N^* when crossing the developer bed, the probability that this particle be still in the background is:

$$p^0_{N^*}(r)=\left[1-p_1(r)\right]^{N^*} \quad (10)$$

Finally, the probability of actually finding in the background a particle of radius comprised between r and $r+dr$ is obtained by multiplying the conditional probability in Eq. 10 by the probability $g(r)dr$ of getting such particle. Thus, the distribution density of toner size in background is:

$$f(r)=\frac{g(r)\left[1-p_1(r)\right]^{N^*}}{\int_0^\infty g(r)\left[1-p_1(x)\right]^{N^*}dx} \quad (11)$$

where the denominator, which serves to normalize the probability of particles with radius r, is a measure of the overall background that results from particles of all possible radii within the distribution.

Note that Eq. 11 relates the size distribution of background toner to that of fresh toner.

Super-Critical Speed

In Mode 4, there are now two distinct cases where a captive particle is detached in one single collision.

- For any incident particle P2 with radius $R > R_2$, the captive particle P1 is readily scavenged and P2 is massive enough to itself escape background, still moving in the same direction. The probability of such event is given by the same equation as Eq. 8 above.
- For any incident particle P2 with radius such that $R_0 < R < R_1$, the captive particle P1 is scavenged as well, but now P2 is not massive enough to continue moving in the same direction. It bounces backward with enough speed to escape background but with reversed motion. We propose the assumption that, as its reverse speed, relatively to the media, tends to vanish due to air drag and possible impacts with other free particles still moving in the original direction, such particle tends to be pulled along in the air boundary layer of the fast moving media, and eventually ends up recaptured by background. This assumption, if correct, provides the basis for an explanation of the observed 'secondary' background. In this perspective, 2 u_0 would be nothing else but the experimentally observed 'critical' speed u_c. If we further assume that later re-deposition of the airborne particles occurs with probability k (determination of k is out of the scope of this paper), then the probability of a particle of radius r generating secondary background is:

$$p_1(r)=k\int_{R_0(r)}^{R_1(r)} g(x)dx \quad (12)$$

where $R_0(r)$ and $R_1(r)$ are given by Eq. 4 and Eq. 5.

Numerical

We assume typical magnetographic monocomponent toners with $\rho_0 = 1000$ kg/m^3, $\eta = 9\%$, $J_0 = 360$ kA/m, and a recording media layer of permeability $\mu = 6$. Then, Eq. 2 yields an escape velocity $u_0 = 0{,}34$ m/s.

We further assume 3 typical toner size distributions, say 'fine, 'medium' and 'coarse', as defined in Table 1 and illustrated in Figure 2.

Table 1. Typical toner particle size distributions

Size 2r	Mean Size	log-normal law parameters	
		λ	τ
Fine	8.3 µm	2.08	0.25
Medium	10.6 µm	2.30	0.33
Coarse	13.3 µm	2.48	0.45

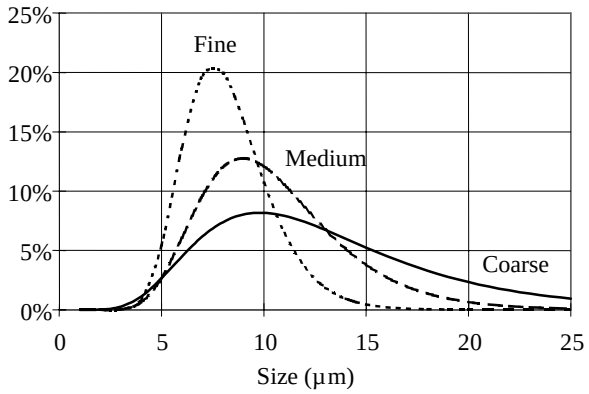

Figure 2. Typical particle size distribution associated with Table 2

Table 2 gives the average size for toner trapped in background, as predicted from Eq. 11, for 3 speeds, respectively 0.35 m/s (close to minimum viable speed), 0.50 m/s (medium sub-critical speed), 0.65 m/s (close to critical speed), as well as a background index arbitrarily taken as the denominator of Eq. 11, such index being 100% for the maximum background which would be generated at speeds lower than the minimum viable speed.

Table 2. Background index and average size of toner in background for sub-critical speeds

	Fine 8,3 µm	Medium 10,6 µm	Coarse 13,3 µm
0.35 m/s	99.3% 8.3 µm	95.4% 10.8 µm	87.8% 13.0 µm
0.50 m/s	24.6% 10.9 µm	19.1% 15.9 µm	30.0% 18.2 µm
0.65 m/s	9.4% 12.3 µm	8.6% 18.0 µm	19.3% 19.9 µm

We see from Table 2 that the background index decreases significantly with increasing speed for all 3 toner size distributions. At the lowest operational speed of 0.35 m/s, the average size of toner in background is practically identical to that of fresh toner, but the narrower size distribution of the 'fine' toner happens to produce higher background than wider ones. As speed increases, there is a general shift toward coarses in the size of background toner, while the trend becomes inverted as concerns the

distribution width; i.e., the wider distribution associated with 'coarse' toner now produces significantly more background than the narrower ones.

Table 3. Background index and average size of toner in background for super-critical speeds

Assume $k = 0.5$	Fine 8,3 µm	Medium 10,6 µm	Coarse 13,3 µm
1,00 m/s	12.2% 10.7 µm	12.2% 14.5 µm	16.9% 18.8 µm
2.00 m/s	19.1% 9.9 µm	19.3% 13.1 µm	19.4% 16.7 µm
3.00 m/s	21.2% 9.8 µm	21.5% 12.9 µm	21.0% 16.2 µm

At super-critical speeds (Table 3), there is little primary background left, but secondary background becomes a factor and is responsible for total background to resume increasing. Also, the average size of toner in background tends to decrease as speed goes up, but remains larger than in fresh toner.

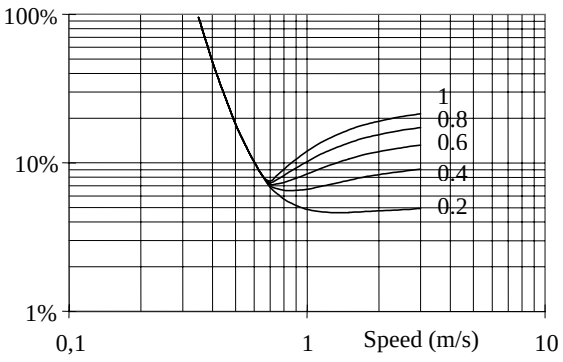

Figure 3. Background index as a function of speed for various recapture probability of secondary background

Figure 3 is a plot of the background index for medium size toner, over a complete speed range going from the minimum operating speed to well over the critical speed, and for various probability values *k* of recapturing airborne particles ($k = 0.2$ to 1 by 0.2 increment).

Experimental

Historically, the first commercial magnetic printer, the Bull MP6090, had a speed of 0.32 m/s; i.e., right in the range 0.28-0.34 predicted by Eq. 2 for minimum operating speed if the media permeability is between 3 and 6. As a matter of fact it has proved very difficult since then to come up with lower speed products because of heavy background.

At same low speed, experimentation had led to the observation (once considered paradoxal) that, on one hand, toner in background had just about the same distribution as fresh toner,[4] while, on the other hand, finer toner always produced more background. This was nothing but the results of Table 2 for low sub-critical speed.

Later on, as faster and faster models were tested, the so-called critical speed was always encountered, generally between 100 and 150 feet/minute[1]; i.e., a 0.5-0.8 m/s range exactly centered on the predicted 0.56-0.68 range. Table 4 indicates how the predicted rate of decrease in the background index at sub-critical speed compares to reported actual background measurements[1].

Table 4. Rate of decrease of background (sub-critical)

slope of log-log plot	Measured [1]			Modeled		
	Exp.1	Exp.2	Exp.3	Fine	Med.	Coarse
	-3.81	-4.76	-2.66	-3.95	-3.96	-3.45
	avg = -3.74 s.d. = 1.05			avg = -3.45 s.d. = 0,87		

Conclusion

The proposed model of random collisions between captive and free toner particles during development produces results well in line both qualitatively and quantitatively with experimental evidences of magnetic background. The observed minimum and critical speeds are correctly predicted by the model, as well as the rate of decrease of background with speed in sub-critical regime. An explanation has been proposed for the increase of background at super-critical speeds. Still, the model needs to be refined to directly relate absolute background measurement (e.g. reflectance) to the system parameters.

References

1. JJ. Eltgen, Process Speed Dependence of Background Development in Magnetography, *IS&T's 46th Annual Conf.*, 1993, pg. 195-198.
2. JJ. Eltgen, A First Order Model of Magnetography: Asymptotic Trend vs. Design Choices, *IS&T's NIP12 conf. Proceedings*, 1996.
3. JJ. Eltgen, A Simple Predictive Analysis of the Speed Range Potential for Magnetography, *ICPS'98 conf. porceedings*, Antwerp, 1998.
4. G. Gerriet, "Fond sur Papier", *internal report*, non published, 1982

Biography

JJ. Eltgen received his degrees in aerospace sciences from the French ENSAe School (Sup'Aero) in Paris in 1967. He has since been engaged in various R&D activity with Bull Groupe, then Nipson, now a Xeikon company, where he is currently responsible for research and technology. His technical work has primarly focused on the modeling of various aspects of magnetography. He is a member of the IS&T.